ACS APPLIED MATERIALS & INTERFACES

Research Article

www.acsami.org

Evolution of Polyvinylidene Fluoride (PVDF) Hierarchical Morphology during Slow Gelation Process and Its Superhydrophobicity

Xianfeng Li,* Chong Zhou, Runhong Du, Nana Li, Xutong Han, Yufeng Zhang, Shulin An, and Changfa Xiao

School of Materials Science and Engineering, State Key Laboratory of Hollow Fiber Membrane Materials and Processes, Tianjin Polytechnic University, Tianjin 300160, People's Republic of China

ABSTRACT: In the paper, we proposed an evolution process of polyvinylidene fluoride (PVDF) macromolecular aggregation in a mixed solvent through the simple and slow gelation process at room temperature. The mixed solvent is prepared with a room-temperature solvent and a high-temperature solvent. The evolution process can be terminated by quenching and exchanging with nonsolvent in a nonsolvent coagulation bath properly, and then the vivid petal-like nanostructure and microspherulite is formed simultaneously. This hierarchical morphology endows PVDF with superhydrophobic and self-cleaning properties, which is useful to PVDF coating and membrane materials. The evolution processes are investigated through the measurements of differential scanning calorimetry (DSC), X-ray diffraction (XRD). In addition, the rheological properties of solution, dry gel and wet gel, are explored.

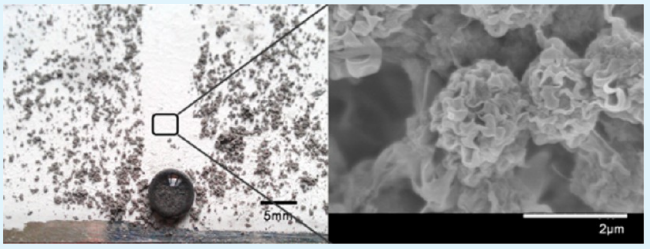

KEYWORDS: *hierarchical morphology, superhydrophobicity, polyvinylidene fluoride (PVDF), spherulite, gelation*

INTRODUCTION

Superhydrophobic and self-cleaning materials have received considerable attention, because of their practical and potential applications in many fields, such as hydrophobic separation membranes, textiles, and automobiles.[1−5] Superhydrophobic and self-cleaning properties rely on the surface morphology of materials if a low surface energy substance is defined.[6] Microhierarchical and nanohierarchical morphologies for low surface energy substance are favorable to superhydrophobicity, because it can provide air pockets.[6−13] Various methods can be used to tailor this hierarchical morphology.[7−13]

With environmental (aging and weathering) stability and the characteristics of crystallization structure, polyvinylidene fluoride (PVDF) has been widely investigated according to its applications of separation membrane, coating, Li-ion separator, and piezoelectric and ferroelectric materials.[14−21] PVDF stands out in various hydrophobic polymer materials, for example, polypropylene (PP), polyethylene (PE), and polytetrafluoroethylene (PTFE), because PVDF materials can be prepared using more techniques (e.g., melt and solution process).

The solution-phase inversion process allows more advantages, such as more-flexible conditions, uniform surface morphology, desired production shape, and simple processing. It includes immersion precipitation (IP), thermally induced phase separation (TIPS), and vapor-induced phase separation (VIPS).[21] Hence, presently, the phase-inversion preparation method of hydrophobic PVDF materials has been comprehensively explored.[21−25] It is difficult to predict the formation of fine morphology for the mechanisms of solution-phase inversion and interactions of macromolecule and solvent are complicated. Although the hierarchical morphology can be formed via blending it with stiff materials, it is very difficult to prepare PVDF superhydrophobic material with vivid hierarchical morphology, because of the softness of polymer and the minimization principle of interfacial energy in the phase-inversion process.[22−25]

Macromolecular aggregates in solution are extremely important to the crystallization morphology of PVDF in the phase-inversion process, which is strongly influenced by solvent types (poor or good solvent) and processing conditions.[26−29] However, only several solvents can be selected to perform a slow crystallization process of PVDF at room temperature. We explored the morphology change of the PVDF membrane prepared with mixed solvent.[18]

In this paper, we proposed an interesting evolution process of PVDF macromolecular aggregates in a mixed solvent via a simple and slow gelation process, which is elaborately designed by mixing a good solvent (a room-temperature solvent) with a good diluent (a high-temperature solvent). The evolution can be terminated by quenching and exchanging with nonsolvent at a proper quenching time point. As a result, the vivid petal-like nanostructure and microspherulite is formed simultaneously, and then the superhydrophobic and self-cleaning material is prepared. The evolution process is investigated through the measurements of differential scanning calorimetry (DSC) and X-ray diffraction (XRD). In addition, the rheological properties of solution, dry gel, and wet gel are explored.

Received: January 14, 2013
Accepted: May 31, 2013
Published: May 31, 2013

EXPERIMENTAL SECTION

Materials. PVDF (low-molecular-weight (solef 6010) and high-molecular-weight (solef 1015)) was supplied by Solvay (France). Dibutyl phthalate (DBP), dioctyl phthalate (DOP), and dimethylacetamide (DMAc) were analytical reagents that were purchased from Tianjin Yongda Chemical Reagent Co. (China).

Samples and Method. The hierarchical morphology surfaces were prepared via natural drying at room temperature after solvent extraction with ethanol. The mixture of 50 vol % DBP in DMAc was used as solvent. PVDF with a proper concentration (15 or 8 wt %) was dissolved in a flask at 100 °C for ~4 h to form a homogeneous solution. The solution was cast into films using a drawknife in a stainless steel plane at 100 °C. The film was gelatinized via quenching in 25 °C air or nonsolvent (ethanol) bath. The film was moved into an ethanol bath to extract the solvent after a specific air quenching time. Ethanol was renewed for several times to remove solvent completely. All the materials and reagents are used without further purification.

Morphology. The hierarchical morphology was observed with a field-emission scanning electron microscopy (FESEM) system (Model 4800, Hitachi, Japan). A cross-section sample was prepared through fracturing in liquid nitrogen. The samples were coated with gold.

X-ray Diffraction (XRD). XRD were performed by Bruker D8 Discover (Germany), and the information was recorded using a general area detector diffraction system (GADDS) in which Cu Kα radiation (λ = 1.5418 Å) was employed.

Differential Scanning Calorimetry (DSC). The sample crystallization of dry and wet gels was characterized by differential scanning calorimetry (DSC) (Model DSC200, Netzsch, Germany). Ascending DSC was obtained at a heating rate of 10 °C/min and descending DSC was measured at a heating rate of 5 °C/min, because of slow crystallization in solution. Approximately 8 mg of sample was sealed in an aluminum pan.

Apparent Contact Angle (ACA). The apparent contact angle (ACA), roll-off, advancing, and receding angles were measured with a contact angle tester (Model DSA100, Krüss, Germany) at room temperature and 50% relative humidity. The deionized water droplet volume was 6 μL when ACA was measured. Their average values were obtained by measuring five different positions.

Rheological Measurement. Rheological properties of the solution were characterized with an Advanced Rheometer AR 2000 system (TA Instruments). The experiments were completed with cone-and-plate geometry on the Peltier plate at a frequency of 6.3 rad/s. The gel was first prepared in a testing tube, and then it was transferred on the Peltier plate. After the temperature rises to 95 °C, the gels were maintained for 5 min. The temperature then decreases at a rate of 10 °C/min.

RESULTS AND DISCUSSION

Figure 1 shows the hierarchical morphologies and the evolution process of PVDF macromolecular aggregates during the gelation process in a DBP/DMAc mixed solvent and an air bath. It can be seen that spherulite cannot be formed in the top surface when the quenching time is short (see Figures 1a and 1b). The sample presents a petal-like supramolecular assembly morphology. The connectivity among assemblies is good. ACA is significantly increased to 141° and 146°, compared with a flat surface (the measured value of 75°).[30] A vivid petal-like assembly and spherulite are formed simultaneously when the quenching time is increased to 300 s (see Figure 1c). The spherulite size is ~2 μm and the thickness of the petal is <50 nm. It is similar to the node morphology of the *Alocasia macrorhiza* leaf, but the size is smaller.[31] This distinct hierarchical morphology endows PVDF with superhydrophobic and self-cleaning properties, as shown in Figure 2. ACA is as high as 158° and the roll-off, advancing, and receding angles attain values of 6°, 160°, and 157°, respectively. A slight tilt leads to sliding of the water droplet. Thus, the dirt on the surface is taken away (Figure 2). The quenching time is further increased to 3 h and a regular spherulite is formed (Figure 1d). Most of the petal-like assemblies then disappear. ACA is maintained at 156° (above 150°). After much longer quenching time (20 days), the spherulitic morphology shows no essential change, compared with the samples treated for 3 h, which are not presented here. Such a simple method lays a good foundation for industrialization.

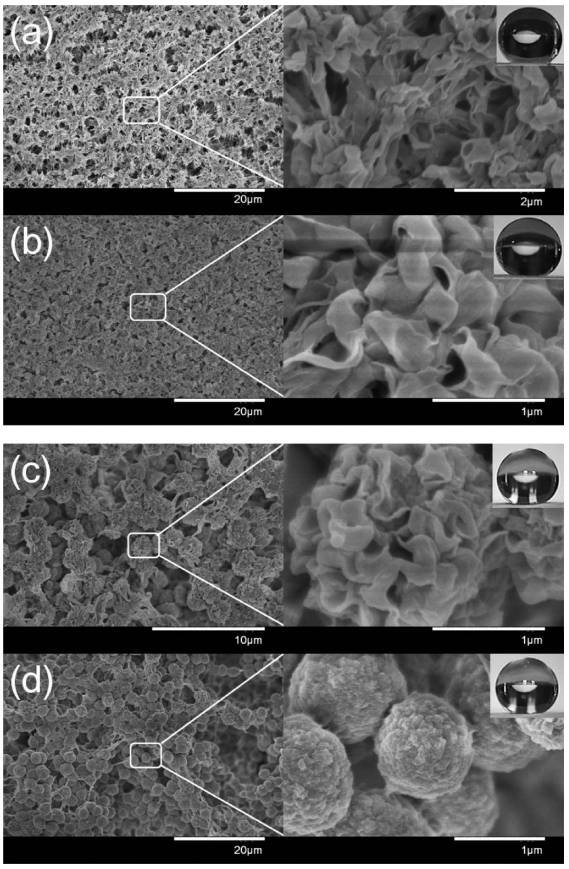

Figure 1. Morphological evolution of the samples prepared with different quenching times from the DBP system (15 wt %): (a) 0 s, (b) 60 s, (c) 300 s, and (d) 3 h.

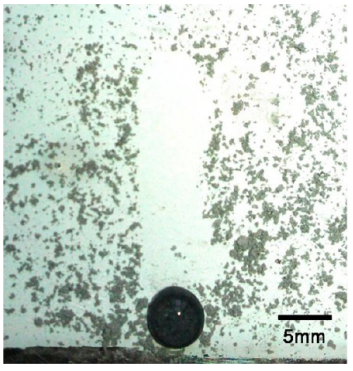

Figure 2. Photograph showing the superhydrophobic and self-cleaning properties of PVDF (15 wt %).

It is well-known that ACA is closely related to the topography for a specific substance.[6] Inherently hydrophilic polymers could be converted to superhydrophobic materials, because of the "geometrical air trapping effect", which is caused by their surface topography.[30,32−34] The theoretical explanation

such a conversion from hydrophility to hydrophobicity was proposed recently.[30,32−34] Actually, the Cassie state to an inherently hydrophilic surface is possible and, moreover, may be stable due to a potential energy barrier between the Cassie and Wenzel wetting states, although it is energetically unfavorable. In this paper, typical microstructured or nanostructured surface is formed when quenching time is 300 s, so air pockets tend to form in the surface. This leads to the highest ACA and a low roll-off angle, although PVDF is inherently a hydrophilic material.[30]

Spherulite morphology is often observed when a polymer crystallizes from the melt or solution without disturbance.[35−39] It is a common crystallization under highly nonequilibrium conditions. The sizes of the spherulites range from micrometers to millimeters, according to the characteristics of the polymer chain and the processing conditions, such as cooling rate, crystallization temperature, and the solution environment (phase inversion mechanism). The structures of the spherulites are similar, regardless of their size, and they are aggregates of crystallites.

In order to investigate the formation of hierarchical morphology, gelation process is characterized via rheological measurement. The storage and loss modulus change of the system during temperature drop is shown in Figure 3 at a fixed

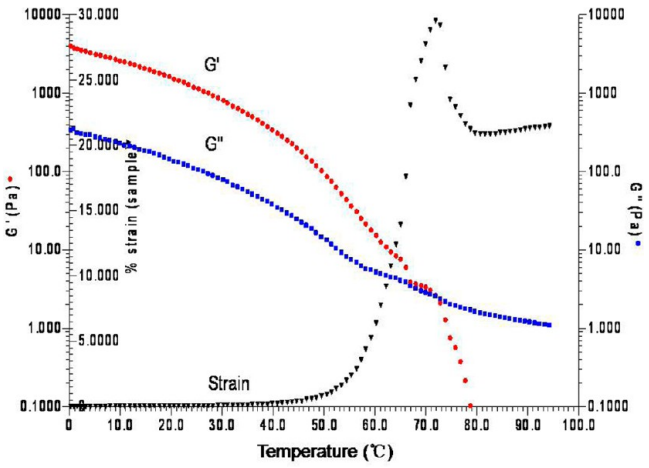

Figure 3. Modulus and strain change of the DBP system, relative to temperature, at a fixed frequency (15 wt %).

frequency. The storage modulus is increased with the decrease of temperature and exceeds the loss modulus at ∼71.8 °C. This shows the transition of solution and gelation, which is confirmed by the peak point of the strain curve. The gradual increase in the modulus indicates the slow gelation process. It seems more similar to PVDF crystallization from a mixed solvent. That is to say, solid−liquid phase inversion occurs to a mixed DBP system. The above results are also found to be consistent with the DSC results, although its crystallization peak is widened (Figure 4a).

The DSC and XRD results of the wet gel (Figure 4) are also examined to obtain gel information. The melt and diffraction peaks of gels show the obvious crystallization of PVDF in the gel. The heating curve of DSC (Figure 4a) indicates that the melt peak is located at ∼71.6 °C. The peak in the cooling curve is wide, even though a low-temperature drop rate is adopted. It shows that the crystallizing rate is slow, because of the mixed-solvent environment. This allows the evolution of PVDF macromolecules at room temperature. The diffraction peaks at 2θ values of 17.9° (100 crystal plane), 18.4° (020 crystal plane), 20.1° (110 crystal plane), and 26.7° (021 crystal plane) are mixed into a strong and widened peak (Figure 4b) with some weak shoulders in the wet gel, and they are almost unable to distinguish.[40,41] This should be the result of the presence of solvent in the wet gel.[42]

Gelation time of the solution with mixed solvent was measured with a simple fluid method (test tube tilting).[15] The measured gelation time ranges from 3.5 h to 18 min when PVDF concentration is changed from 5 wt % to 15 wt %. The gelation time is much longer than that of the solution with pure DBP diluent.[15,35] Based on such a long gelation time, it could be assumed that not only a slow crystallization (solid−liquid phase inversion) is dominant in the gelation process but also a low degree of undercooling occurs when the solution is cooled at room temperature. it is not difficult to understand microspherulite formation from the results of DSC, XRD, the gelation process, and the gelation time.[35−39]

It is very difficult for a polymer to obtain nanostructure, because of its softness and the minimization principle of interfacial energy in the phase-inversion process. However, a vivid petal-like nanostructure in the research is formed in a proper quenching time point. Generally, the formation reasons are related to the interaction among the macromolecule, the solvent, and the nonsolvent (thermodynamics and kinetics). DBP (a good diluent) is usually used as a diluent of PVDF in a TIPS process at high temperature (above 200 °C).[35] DMAc, which is a common solvent, is often used to prepare porous membranes via an IP process. After the two solvents are mixed together, the formed solvent is able to dissolve PVDF at the comparatively lower temperature (100 °C) than the TIPS

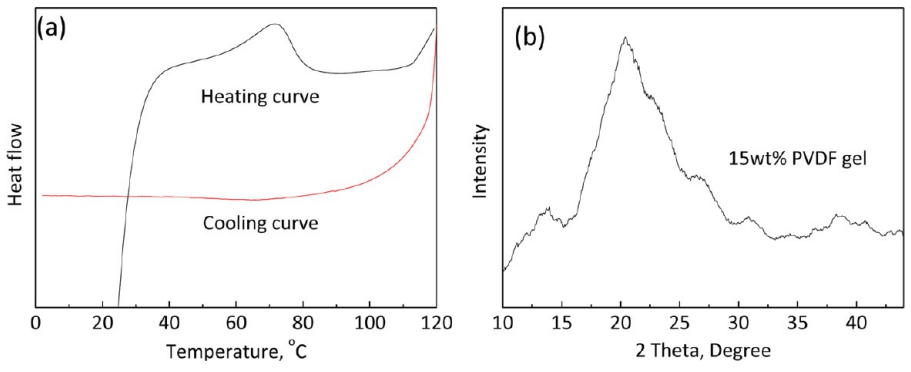

Figure 4. (a) Differential scanning calorimetry (DSC) and (b) X-ray diffractometry (XRD) of wet gel (15 wt %).

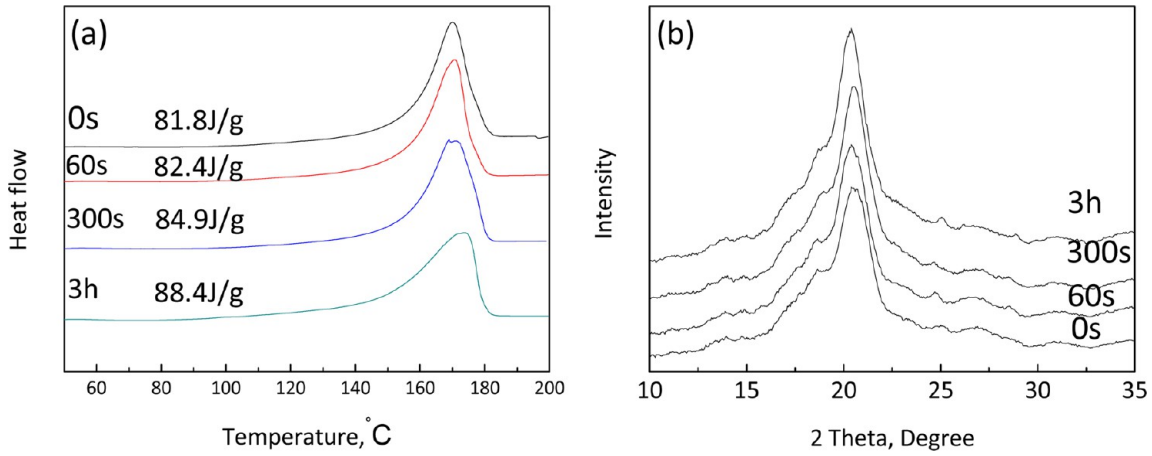

Figure 5. (a) DSC and (b) XRD of dried sample with different quenching time (15 wt %).

process. Moreover, the solution can be gelatinized slowly at room temperature. Therefore, the mixed solvent provides a solvent environment for the aggregation of PVDF macromolecules. Slow aggregation and crystallization conditions in solution will be created due to the poorer DBP solvent environment.[26−29] Room-temperature solvent increases the gelation time of the system. It provides a chance to terminate this evolution in different periods.

The nonsolvent (ethanol) plays a key role in terminating this evolution by quenching and exchanging with the solvent. When the 100 °C solution film is immersed in an ethanol coagulant bath, macromolecular aggregates on the surface are instantaneously solidified because macromolecular aggregates have no time to develop into spherulite, because of quick cooling and the exchange rate. Thus, the petal-like nanoassemblies in the surface are formed. Proper quenching time in air allows the evolution of macromolecular aggregates. Different quenching time leads to different developing extents of macromolecular aggregates. When the quasi-gelation film is deposited into an ethanol coagulation bath, the developing aggregates are instantaneously solidified on the surface of the developing spherulite. As a result, the petal-like nanoassemblies on the surface of spherulite are formed.

The dry samples are measured with DSC and XRD to investigate the crystallization of PVDF. The low-temperature migration of the beginning melt point, the widening of the melt peak, and the increasing of the crystallization heat further indicate the evolution process of PVDF macromolecule aggregates with the increase in quenching time (Figure 5a). The strengthening of diffraction peak (Figure 5b) with quenching time also indicates an increasing crystallinity. More obvious peaks at 2θ = 25° and 26.7°, with the increase of quenching time, show two more perfect crystal planes. Thus, more PVDF macromolecules take part in crystallization or the crystallization process becomes better. As a result, the surface morphology changes with the evolution of macromolecular aggregates. At a proper quenching time point, a vivid hierarchical morphology can be obtained. However, more macromolecules can take part in crystallization and macromolecular chain segments can also be mobilized and reorganized if enough air quenching time is given. Consequently, the vivid nanostructure disappears and a regular spherulite morphology is the result (see Figure 1d). Usually, PVDF can crystallize into α-, β-, or γ-phases via different processes. The similarity of the shape and position of several main diffraction peaks at 2θ = 17.9° (100), 18.4° (020), 20.1° (110), and 26.7° (021) indicate that (i) the crystalline phase does not change with quenching time and (ii) the crystalline α-phase is dominant.[40,41]

Different PVDF concentrations (8 wt %) are adopted to confirm the effectiveness of nanostructure formation via mixed solvent, and the wormlike nanostructure is formed on the surface of microspherulite from a quasi-gelation sample (Figure 6a). It keeps a high ACA of 157°. Although a regular spherulite

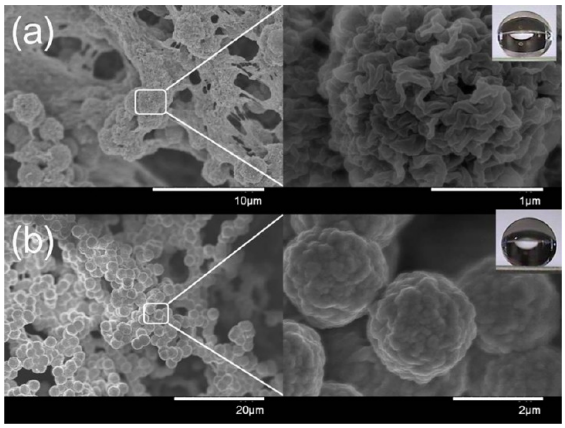

Figure 6. Morphological evolution of the samples prepared with different quenching time (8 wt %): (a) 30 min and (b) 3 h.

(Figure 6b) results after a long quenching time, it is similar to the samples prepared with the PVDF concentration of 15 wt %. The regular spherulite is composed of small particles. The superhydrophobic polypropylene (PP) coating is this morphology, according to the low-magnification photo.[39] However, microspherulite cannot be found from the top surface for high-molecular-weight PVDF (Figure 7). Its ACA is low (137°).

The cooling rate will theoretically affect the aggregation process of PVDF. The higher cooling rate is adopted through depositing the solution film in a sealed metal vessel (0.3 mm thickness wall) in a room-temperature water bath (without direct contact or exchanging with water). A deformed petal-like nanostructure and microspherulite are obtained for both 8 wt % and 15 wt % PVDF concentration and the connectivity among spherulites are enhanced (Figure 8). The two films still present a good hydrophobicity (above 150°).

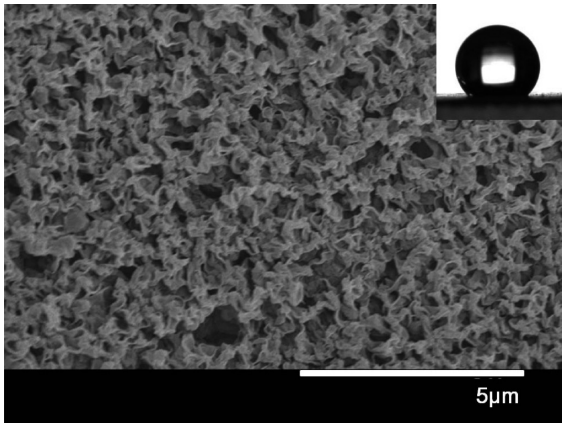

Figure 7. Morphological features of the samples prepared with high molecular weight (8 wt %), 30 min quenching time.

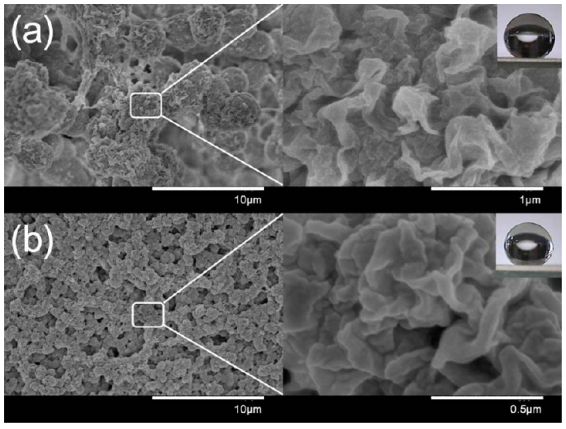

Figure 8. Morphological features of the samples prepared with different concentrations via water bath cooling (30 min): (a) 8 wt % and (b) 15 wt %.

When DBP is changed to its brother, DOP, the morphology and evolution process is abruptly different. The spherulite cannot be formed when the quenching time is within 300 s (Figure 9), while a uniform network morphology is presented. The selection of sample time point is based on the time of solution solidification (or gel time), so three samples (0 s, 30 s before gelation, and 300 s after gelation) are selected in our investigation. Figures 9b and 9c show similar morphologies; thus, the longer quenching time is not necessary. The largest ACA of the three samples is <145°. However, the dense top surface, which often results from immersion precipitation, is avoided, although the spherulite morphology cannot be formed. This still clearly enhances the hydrophobicity of PVDF.

The reasons of morphology formation are investigated via rheological measurement for the DOP/DMAc system. Compared to the DBP/DMAc system, the transition point of solution and gelation rises to 82.6 °C (the peak point of strain curve) and the modulus increases rapidly to a stable value when the temperature decreases (see Figure 10). It shows a shorter

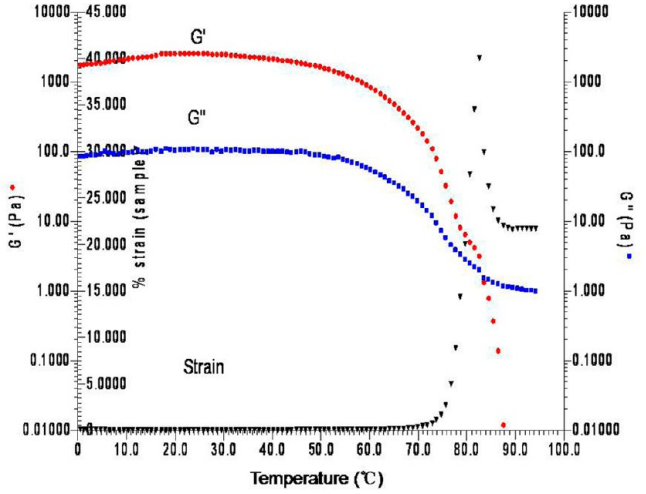

Figure 10. Modulus and strain change with temperature at a fixed frequency (15 wt %; DOP system).

gelation time, compared to the DBP/DMAc system, which is validated by the fast gelation in the fluid test process. DOP has poorer diluents than DBP, and then the DOP mixed solvent becomes poorer than the DBP mixed system. It should be speculated that liquid–liquid phase inversion may occur for the DOP system, according to the results of rheological measurement and the shorter gelation time. The shorter gelation time and poorer solvent is unfavorable to macromolecule mobility into spherulite, so the network structure is obtained. The detailed reasons require further experiments.

CONCLUSION

Mixed solvent creates the conditions that allow the evolution of PVDF macromolecular aggregates in solution at room temperature, which is favorable to the formation of a hierarchical morphology. Various microscale and nanoscale hierarchical morphologies can be fabricated via termination of the evolution process by quenching and exchanging with a nonsolvent. Superhydrophobic and self-cleaning properties then are endowed with PVDF materials. In addition, the gelation process can be implemented at room temperature, and the gelation time can be extended with good solvent in a mixed solvent. The features are beneficial to the industrialization.

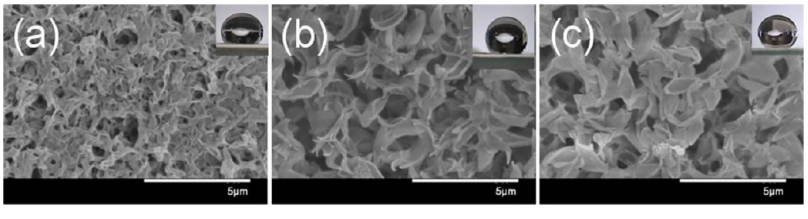

Figure 9. Morphological evolution of the samples prepared with different quenching times from the DOP system (15 wt %): (a) 0 s, (b) 30 s, and (c) 300 s.

AUTHOR INFORMATION

Corresponding Author

*Tel.: 86-22-83955809. Fax: 86-22-83955055. E-mail: xianfengli022@gmail.com.

Notes

The authors declare no competing financial interest.

ACKNOWLEDGMENTS

The authors thank the National Basic Research Development Program of China (973 Program, No. 2012CB722706), the National Natural Science Foundation of China (No. 51073120), and the Scientific Research Foundation for the Returned Overseas Chinese Scholars, State Education Ministry.

REFERENCES

(1) Honeychuck, R. V.; Ho, T.; Wynne, K. J.; Nissan, R. A. *Chem. Mater.* **1993**, *5*, 1299−1306.
(2) Genzer, J.; Efimenko, K. *Biofouling* **2006**, *22*, 339−360.
(3) Rajabzadeh, S.; Yoshimoto, S.; Teramoto, M.; Al-Marzouqib, M.; Matsuyama, H. *Sep. Purif. Technol.* **2009**, *69*, 210−220.
(4) Wang, K. Y.; Chung, T. S.; Gryta, M. *Chem. Eng. Sci.* **2008**, *63*, 2587−2594.
(5) Khayet, M. *Adv. Colloid Interface Sci.* **2011**, *164*, 56−88.
(6) Yang, C.; Tartaglino, U.; Persson, B. N. J. *Phys. Rev. Lett.* **2006**, *97*, 116103-1−116103-4.
(7) Barthlott, W.; Neinhuis, C. *Planta* **1997**, *202*, 1−8.
(8) Pastine, S. J.; Okawa, D.; Kessler, B.; Rolandi, M.; Llorente, M.; Zettl, A.; Fréchet, J. M. J. *J. Am. Chem. Soc.* **2008**, *130*, 4238−4239.
(9) Nakanishi, T.; Michinobu, T.; Yoshida, K.; Shirahata, N.; Ariga, K.; Möhwald, H.; Kurth, D. G. *Adv. Mater.* **2008**, *20*, 443−446.
(10) Wang, J.; Shen, Y.; Kessel, S.; Fernandes, P.; Yoshida, K.; Yagai, S.; Kurth, D. G.; Möhwald, H.; Nakanishi, T. *Angew. Chem., Int. Ed.* **2009**, *48*, 2166−2170.
(11) Park, S. H.; Lee, S. M.; Lim, H. S.; Han, J. T.; Lee, D. R.; Shin, H. S.; Jeong, Y.; Kim, J.; Cho, J. H. *ACS Appl. Mater. Interfaces* **2010**, *2*, 658−662.
(12) Broderick, A. H.; Manna, U.; Lynn, D. M. *Chem. Mater.* **2012**, *24*, 1786−1795.
(13) Deng, X.; Mammen, L.; Butt, H.-J.; Vollmer, D. *Science* **2012**, *335*, 67−70.
(14) Bottino, A.; Camera-Roda, G.; Capannelli, G.; Munari, S. *J. Membr. Sci.* **1991**, *57*, 1−20.
(15) Yadav, P. J. P.; Ghosh, G.; Maiti, B.; Aswal, V. K.; Goyal, P. S.; Maiti, P. *J. Phys. Chem. B* **2008**, *112*, 4594−4603.
(16) Cheng, L. P. *Macromolecules* **1999**, *32*, 6668−6674.
(17) Choi, S. W.; Jo, S. M.; Lee, W. S.; Kim, Y. R. *Adv. Mater.* **2003**, *15*, 2027−2032.
(18) Li, X. F.; Wang, Y. G.; Lu, X. L.; Xiao, C. F. *J. Membr. Sci.* **2008**, *320*, 477−482.
(19) Gugliuzza, A.; Drioli, E. *Desalination* **2009**, *240*, 14−20.
(20) Li, C.-L.; Wang, D.-M.; Deratani, A.; Quémener, D.; Bouyer, D.; Lai, J.-Y. *J. Membr. Sci.* **2010**, *361*, 154−166.
(21) Liu, F.; Hashim, N. A.; Liu, Y.; Abed, M. R.; Li, K. *J. Membr. Sci.* **2011**, *375*, 1−27.
(22) Zha, D.; Mei, S.; Wang, Z.; Li, H.; Shi, Z.; Jin, Z. *Carbon* **2011**, *49*, 5166−5172.
(23) Zhang, L.; Zha, D.; Du, T.; Mei, S.; Shi, Z.; Jin, Z. *Langmuir* **2011**, *27*, 8943−8949.
(24) Schutzius, T. M.; Bayer, I. S.; Tiwari, M. K.; Megaridis, C. M. *Ind. Eng. Chem. Res.* **2011**, *50*, 11117−11123.
(25) Razmjou, A.; Arifin, E.; Dong, G.; Mansouri, J.; Chen, V. *J. Membr. Sci.* **2012**, *415*, 850−863.
(26) Raos, G.; Allegra, G. *J. Chem. Phys.* **1997**, *107*, 6479−6490.
(27) Heckmeier, M.; Mix, M.; Strobl, G. *Macromolecules* **1997**, *30*, 4454−4458.
(28) Hong, P.-D.; Chou, C.-M.; He, C. H. *Polymer* **2001**, *42*, 6105−6112.
(29) Tucker, A. K.; Stevens, M. J. *Macromolecules* **2012**, *45*, 6697−6703.
(30) Bormashenko, E.; Stein, T.; Whyman, G.; Bormashenko, Y.; Pogreb, R. *Langmuir* **2006**, *22*, 9982−9985.
(31) Koch, K.; Barthlott, W. *Philos. Trans. R. Soc. A* **2009**, *367*, 1487−1509.
(32) Whyman, G.; Bormashenko, E. *Langmuir* **2011**, *27*, 8171−8176.
(33) Bormashenko, E.; Bormashenko, Y.; Whyman, G.; Pogreb, R.; Stanevsky, O. *J. Colloid Interface Sci.* **2006**, *302*, 308−311.
(34) Herminghaus, S. *Europhys. Lett.* **2000**, *52*, 165−170.
(35) Li, X. F.; Lu, X. L. *J. Appl. Polym. Sci.* **2006**, *101*, 2944−2952.
(36) Keith, H. D.; Padden, F. J. *Polymer* **1986**, *27*, 1463−1471.
(37) Goldenfeld, N. *J. Cryst. Growth* **1987**, *84*, 601−608.
(38) Magill, J. H. *J. Mater. Sci.* **2001**, *36*, 3143−3164.
(39) Erbil, H. Y.; Demirel, A. L.; Avci, Y.; Mert, O. *Science* **2003**, *299*, 1377−1380.
(40) Lovinger, A. J.; Wang, T. T. *Polymer* **1979**, *20*, 725−732.
(41) Steinhart, M.; Senz, S.; Wehrspohn, R. B.; Gösele, U.; Wendorff, J. H. *Macromolecules* **2003**, *36*, 3646−3651.
(42) Yadav, P. J. P.; Maiti, B.; Ghorai, B. K.; Sastry, P. U.; Patra, A. K.; Aswal, V. K.; Maiti, P. *Macromolecules* **2011**, *44*, 3029−3038.